



# Synthesis and Evaluation of Levulinic Ester as Biodiesel Additives

ELENA-EMILIA OPRESCU<sup>1,2</sup>, CRISTINA-EMANUELA ENASCUTA<sup>1\*</sup>, ELENA RADU<sup>1</sup>, VASILE LAVRIC<sup>1,3</sup>

<sup>1</sup>National Research & Development Institute for Chemistry and Petrochemistry-ICECHIM, 202 Splaiul Independentei, 060021, Bucharest, Romania

<sup>2</sup>Petroleum-Gas University of Ploiesti, 39 Bucuresti Blvd., 100680 Ploiesti, Romania

<sup>3</sup>University Politehnica Bucharest, Faculty of Applied Chemistry and Materials Science, 1-7 Polizu Str., 011061, Bucharest, Romania

**Abstract.** In this study, the  $SO_4^{2-}/TiO_2-La_2O_3-Fe_2O_3$  catalyst was prepared and tested in the conversion of fructose to ethyl levulinate. The catalyst was characterized from the point of view of the textural analysis, FT-IR analysis, acid strength distribution, X-ray powder diffraction and pyridine adsorption IR spectra. The influence of the reaction parameters on the ethyl levulinate yield was studied. The maximum yield of 37.95% in levulinate esters was obtained at 180 °C, 2 g catalyst and 4 h reaction time. The effect of ethyl levulinate addition to diesel-biodiesel blend in different rates, i.e. 0.5, 1, 2.5, 5 (w.t %) on density, kinematic viscosity and flash point was evaluated and compared with the European specification.

**Keywords:** ethyl levulinate, superacid, additives, biodiesel

## 1. Introduction

Biodiesel is the best known “green fuel” due to its biodegradable, renewable, non-toxic and environmental friendly properties [1]. However, it has some disadvantages when is used at low temperatures due to its high viscosity, cloud point and pour point.

To resolve these and other problems is required utilization of fuel additives. Diesel engines have negative effects on the environment due to high exhaust emissions. To eliminate these effects, an alternative method is adding additives (oxygenates) to conventional fuels. In this context, the use of ethyl levulinate as additive for biofuels provides a longer engine life as well as reduced emissions of carbon monoxide and nitrogen oxide.

Alkyl levulinates such as ethyl levulinate or methyl levulinate are known as oxygenated fuel additives due to their high ignition temperature properties, oxygen content and clean combustion [2,3]. For exemple, ethyl levulinate added in diesel fuel up to 5% has excellent properties, such as clean combustion and low toxicity [4].

Methyl levulinate and ethyl levulinate obtained by esterification of levulinic acid with short alcohols over different types of acid catalysts can be used as fuel additives or can partial replace petroleum-derived chemical feedstocks. Compared to homogeneous catalysts, the heterogeneous catalysts are reusable, non-corrosive and eliminate the neutralization step which leads to formation of waste water [5]. Yadav et al. prepared and tested a series of catalysts based on sulphated metal oxide in the synthesis of ethyl levulinate. The results indicated that the most active catalyst was the mesoporous super acidic zirconia. To establish the kinetics and mechanism of reaction under optimized conditions, the effects of various parameters were studied [6].

This paper reports the synthesis of ethyl levulinate over a ferromagnetic solid superacid catalyst  $SO_4^{2-}/TiO_2-La_2O_3$ . The influence of the reaction parameters on the ethyl levulinate yield such as catalyst weight, temperature and reaction time were studied.

\*email: [cristina.enascuta@gmail.com](mailto:cristina.enascuta@gmail.com)



The characteristics of diesel blends containing biodiesel and different percent of ethyl levulinate, focusing our interest on density, viscosity and flash point properties were valuated.

## 2. Materials and methods

### 2.1. Chemicals

All reagents used were analytical grade and purchased from Sigma-Aldrich.

### 2.2. Catalyst preparation

The  $\text{SO}_4^{2-}/\text{TiO}_2\text{-La}_2\text{O}_3\text{-Fe}_2\text{O}_3$  catalyst was prepared in three steps. Firstly, the  $\text{Fe}_3\text{O}_4$  nanoparticles were prepared by co-precipitation method [7]. In the second step, the  $\text{TiO}_2\text{-La}_2\text{O}_3\text{-Fe}_2\text{O}_3$  support is prepared by dripping titanium butoxide into an alcoholic solution containing lanthanum salt (0.93 g) and ferromagnetite (2.5 g), under vigorous stirring and heated at  $70^\circ\text{C}$  for 12 h. The resulting solid was separated by a magnet, washed and dried at  $110^\circ\text{C}$  for 24 h. In the last step, the obtained support is impregnated with a solution of 1M sulfuric acid under sonification and then separated, dried and calcined at  $480^\circ\text{C}$  for 4h.

### 2.3 Synthesis of ethyl levulinate

All experiments were performed in a Parr autoclave with a capacity of 600 mL with control module 4843. In a typical experiment, the autoclave is loaded with the reaction mixture consisting of: fructose, catalyst and ethanol. The working parameters (temperature, pressure and agitator speed) were set by a controller. After completion of the reaction, the mixture is filtered to remove the catalyst. In the next step, the filtrate is subjected to the distillation process to remove excess of ethyl alcohol that can be reused in subsequent experiments. The distillation was performed in the temperature range between  $65\text{-}71^\circ\text{C}$ , at atmospheric pressure using a rotary evaporator. The distillate was subjected to GC-MS analysis.

### 2.4. Product analysis

The reaction products were analyzed using a TRIPLE QUAD GC-MS / MS type gas chromatograph (Agilent 7890 A) fitted with a DB-WAX capillary column (length 30 m, internal diameter 0.25 mm, film thickness 0, 25  $\mu\text{m}$ ) and helium as carrier gas at a flow rate of 1 mL / min. The temperature program was as follows:  $70^\circ\text{C}$ ,  $7^\circ\text{C}/\text{min}$  up to  $270^\circ\text{C}$ , 5 min holding time. The temperature of the GC injector and the MS ion source were  $250^\circ\text{C}$  and  $150^\circ\text{C}$ , respectively. The transfer line temperature was  $280^\circ\text{C}$ . The MS detector was operated in EI mode at 70 eV, with a range scanning  $m/z$  of 50–450 [8].

### 2.5. Catalyst characterization

The  $\text{SO}_4^{2-}/\text{TiO}_2\text{-La}_2\text{O}_3$  catalyst supported on the ferromagnetite was characterized from the point of view of the textural analysis and acid strength distribution by diethylamine thermodesorption. The textural characteristics were determined using a NOVA 2200e-Quantachrome Analyzer porosimeter, while the DuPont Instruments "Thermal Analyst 2000/2100" coupled with a "951 Thermogravimetric Analyzer" module was used to determine the acidity [9]. X-ray diffraction (XRD) analysis was carried out using Bruker D8 Advance X-ray diffractometer with  $\text{Cu}\cdot\text{K}\alpha$  radiation ( $\lambda_{\text{Cu}} = 1.5406 \text{ \AA}$ ) operating at 40 kV and 40 mA. Data were collected in  $2\theta$  range from  $10.0^\circ$  to  $70^\circ$ , with a scanning rate of  $0.2 \text{ deg} \cdot \text{min}^{-1}$ . Fourier transform infrared (FT-IR) spectroscopy analysis was recorded in the range  $4000\text{-}400 \text{ cm}^{-1}$  using FT-IR Tensor 27 - Bruker spectrometer employing KBr pellet technique [10].

## 2.6 Diesel blends characterization

The European standards used to characterize the mixtures of diesel, biodiesel and ethyl levulinate were: SR EN ISO 12185/02 (density at 20°C); EN ISO 3104 (kinematic viscosity at 40°C), EN ISO 3016 (pour point), SR EN ISO2592 (flash point).

## 3. Results and discussions

### 3.1 Catalyst characterization

Concerning to the diffusion rate of the reactants and reaction products into and from the pores, the specific surface area, pore volume and average pore diameter were determined [9]. The textural characteristics indicate the obtaining of mesoporous structure, a fact confirmed by the specific surface value of 109.28 m<sup>2</sup>/g, as well as by the average pore diameter of 5.47 nm and the total pore volume of 0.168 cm<sup>3</sup>/g.

The FT-IR analysis was used to confirm the impregnation of sulfated functional groups on TiO<sub>2</sub>-La<sub>2</sub>O<sub>3</sub>-Fe<sub>2</sub>O<sub>3</sub> support (Figure 1).

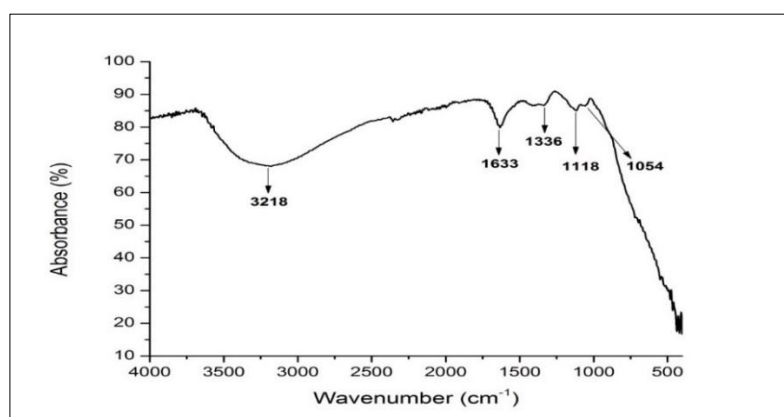


**Figure 1.** Infrared spectra of SO<sub>4</sub><sup>2-</sup>/TiO<sub>2</sub>-La<sub>2</sub>O<sub>3</sub>-Fe<sub>2</sub>O<sub>3</sub>

The absorption peaks around 3218 cm<sup>-1</sup> and 1633 cm<sup>-1</sup> are associated with the bending and stretching vibrations of the OH group of water molecules on the surface of the solids and with terminal OH which are characteristic of metal oxides. The characteristic bands of the stretching modes of sulfate groups impregnated on SO<sub>4</sub><sup>2-</sup>/TiO<sub>2</sub>-La<sub>2</sub>O<sub>3</sub>-Fe<sub>2</sub>O<sub>3</sub> were observed in the region of 1193 - 989 cm<sup>-1</sup>. The IR absorption bands at 1054, 1118 and 1336 cm<sup>-1</sup> are assigned to the typical bands of chelating bidentate sulfate ion coordinated to TiO<sub>2</sub>-La<sub>2</sub>O<sub>3</sub>-Fe<sub>2</sub>O<sub>3</sub> support [11].

FT-IR spectroscopy of adsorbed pyridine was used for Brønsted and Lewis acid sites identification. The FT-IR spectra of pyridine adsorbed on SO<sub>4</sub><sup>2-</sup>/TiO<sub>2</sub>-La<sub>2</sub>O<sub>3</sub>-Fe<sub>2</sub>O<sub>3</sub> (Figure 2) presents characteristics bands assign to both Brønsted and Lewis acid sites. The bands at 1539 and 1636 cm<sup>-1</sup> are correlated with Brønsted acid sites, whereas the band at 1487 cm<sup>-1</sup> corresponds to a peak attributed to both Brønsted and Lewis acid sites. These results are in accordance with previous studies [12].

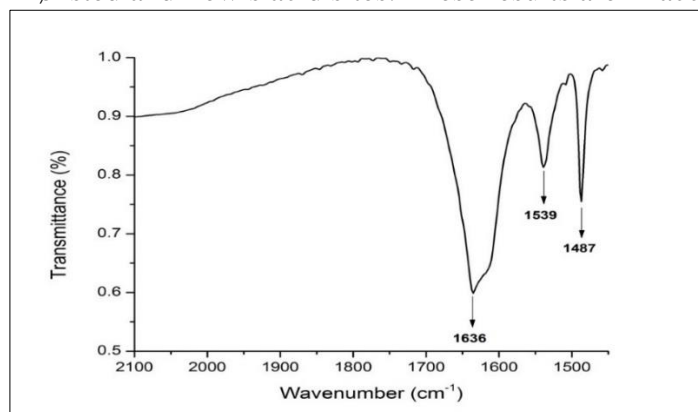


**Figure 2.** Infrared spectra of adsorbed pyridine on SO<sub>4</sub><sup>2-</sup>/TiO<sub>2</sub>-La<sub>2</sub>O<sub>3</sub>-Fe<sub>2</sub>O<sub>3</sub>

The distribution of acid centers was calculated on the basis of the thermosorption curve of diethylamine. The acidic sites were categorized into three types: weak, intermediate and strong acid sites based on diethylamine desorption temperature (100-240°C, 240-340°C and respectively 340-500°C) [13]. From the recording data (Figure 3) it can be seen balanced relationship between weak (0.39 mEq/g), medium (0.38 mEq/g) and strong acid centers (0.29 mEq/g). The total acidity of the catalyst calculated was of 1.06 mEq/g.

The XRD pattern of  $\text{SO}_4^{2-}/\text{TiO}_2\text{-La}_2\text{O}_3\text{-Fe}_2\text{O}_3$  catalyst is present in Figure 4. It can be seen that  $\text{SO}_4^{2-}/\text{TiO}_2\text{-La}_2\text{O}_3\text{-Fe}_2\text{O}_3$  exhibit mainly the crystalline form of anatase with peaks at  $2\theta = 25^\circ, 38^\circ, 48^\circ, 54^\circ$  and  $66^\circ$  indicating the presence of only the tetragonal phase [11]. Iron oxide, specific peaks can be observed at  $2\theta \approx 30^\circ$  and  $36^\circ$  [14]. Moreover, no crystalline phase determined by the presence of  $\text{La}_2\text{O}_3$  was identified on the catalyst surface.

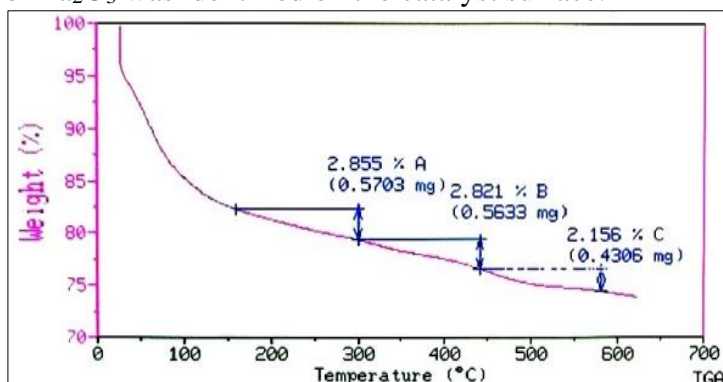


**Figure 3.** Acid strength distribution of the  $\text{SO}_4^{2-}/\text{TiO}_2\text{-La}_2\text{O}_3\text{-Fe}_2\text{O}_3$

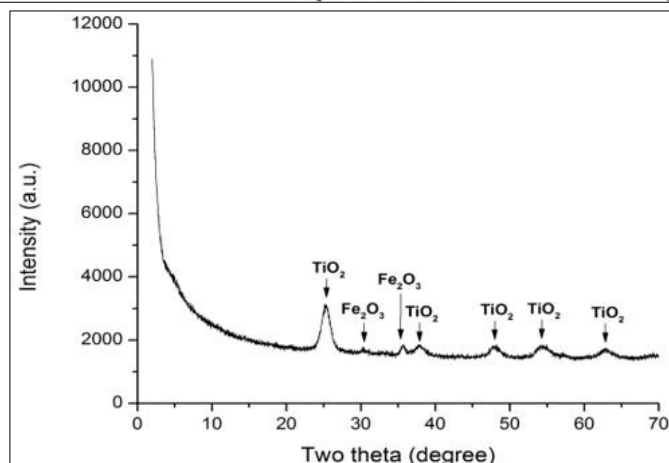


**Figure 4.** X-ray powder diffraction (XRD) spectrum of  $\text{SO}_4^{2-}/\text{TiO}_2\text{-La}_2\text{O}_3\text{-Fe}_2\text{O}_3$

### 3.2 Effect of reaction parameters

The influence of the reaction parameters on the yield of ethyl levulinate is shown in Table 1. The technological parameters studied for optimization were: the mass ratio of the catalyst, the reaction time and the reaction temperature.

The effect of the reaction temperature was studied in the temperature range 150-210°C. The experimental results indicate a strong dependence between this parameter and the yield of ethyl levulinate. The maximum yield in ethyl levulinate was reached at 180°C. This result suggests that the higher temperature favors the conversion of fructose to ethyl levulinate. In addition, there is a decrease in 5-ethoxymethyl furfural content (the secondary compound obtained), which means that most of this compound has been converted to ethyl levulinate. Thus, the 5-ethoxymethyl furfural compound is considered to be intermediate in the synthesis of ethyl levulinate by cleavage of the carbonyl group on the furfural ring with the formation of levulinic acid which is immediately converted to ethyl levulinate. At higher temperature, such as 210°C, a slightly decrease in the yield of ethyl levulinate was observed. The time evolution of the ethyl levulinate yield tends to increase continuously. After a



reaction time of 4 h, the yield remains almost constant. In view of the results obtained, the optimum reaction time was selected at 4 h. Another parameter evaluated was the influence of catalyst mass. The experimental results obtained indicate a strong effect over the levulinic ester yield, leading to an increase of yield values as the catalyst mass increased. The maximum value of 37.95% yield in ethyl levulinate was reached at 2 g of catalyst. This variation can be explained by an increase in the number of acidic groups which due to high polarity improve the accessibility of the reactant molecules to the catalytic acid centers.

**Table 1.** Experimental results of the ethyl levulinate synthesis

Entry	Time reaction (h)	Reaction temperature (°C)	Catalyst mass (g)	Ethyl levulinate yield (%)
1	1	150	0.5	7.01
2	2	150	1	10.54
3	3	150	1.5	15.87
4	4	150	2	15.25
5	1	180	0.5	19.52
6	2	180	1	23.95
7	3	180	1.5	32.65
8	4	180	2	37.95
9	1	210	0.5	24.23
10	2	210	1	31.86
11	3	210	1.5	34.45
12	4	210	2	38.25

### 3.3. Fuel blend properties

The notation used are: *P<sub>0</sub>* for between diesel and biodiesel (7 wt.%), *P<sub>i</sub>* for blends consist of diesel, biodiesel and ethyl levulinate. The value of index *i* correspond to ethyl levulinate percent in diesel and biodiesel blends (*i. e.* 0.5, 1, 2.5 and 5 wt. %). The experimental results are presented in Table 2. The data presented in Table 2 show an increase of density with the increasing of ethyl levulinate content from 0,8462 to 0,8506 g/cm<sup>3</sup>. The viscosity increases from 2.6873 mm<sup>2</sup>/s for 0.5 wt. % of ethyl levulinate to 2.7850 mm<sup>2</sup>/s for 1 wt. % additive, after which decreases to 2.6858 mm<sup>2</sup>/s for 5 wt. % of ethyl levulinate. This variation is in accordance with literature data [15,16]. The volatility and flammability of the compounds added to diesel considerably influence the flash point of the mixture. The experimental data obtained indicate a decrease in flash point values from 68°C for 0,5% by weight of additive to 58 °C for 5% by weight of ethyl levulinate.

**Table 2.** Characteristics of the fuel blends

Entry	Sample	Density, d <sub>4</sub> <sup>20</sup>	Viscosity at 40°C, mm <sup>2</sup> /s	Flash point, °C
1	P <sub>0</sub>	0.8462	2.6715	72
2	P <sub>0.5</sub>	0.8489	2.6873	68
3	P <sub>1</sub>	0.8459	2.7850	66
4	P <sub>2.5</sub>	0.8477	2.7254	62
5	P <sub>5</sub>	0.8506	2.6858	58

## 4. Conclusions

The synthesis of ethyl levulinate in one step over SO<sub>4</sub><sup>2-</sup>/TiO<sub>2</sub>-La<sub>2</sub>O<sub>3</sub> catalyst supported on the ferromagnetite was investigated. The prepared catalyst was characterized by FT-IR analysis, BET analysis and acid strength distribution. The influence of reaction temperature, reaction time and catalyst amount on ethyl levulinate yield was studied. The GC-MS/MS method was used for identification of the obtained compounds. The maximum yield of 37.95% in levulinate esters was obtained at 180°C, 2 g catalyst and 4 h reaction time. The influence of ethyl levulinate on the diesel-biodiesel blends properties like viscosity, pour point and flash point was studied.



**Acknowledgments:** The authors gratefully acknowledge the financial support of the UEFISCDI, Romania, in the framework of National Partnership Program, financing contract no. 104 PD/2018.

## References

1. UNLU, D., OGUZHAN ILGEN O., HILMIOGLU N., Biodiesel additive ethyl levulinate synthesis by catalytic membrane:  $\text{SO}_4^{2-}/\text{ZrO}_2$  loaded hydroxyethyl cellulose, *Chem. Eng. J.*, **302**, 2016, p. 261.
2. NANDIWALE, K., SONAR, S., NIPHADKAR, P., JOSHI, P., DESHPANDE, S., PATIL, V., BOKADE, V., Catalytic upgrading of renewable levulinic acid to ethyl levulinate biodiesel using dodecatungstophosphoric acid supported on desilicated H-ZSM-5 as catalyst, *Appl. Catal. A Gen.*, **460–461**, 2013, p. 92.
3. NANDIWALE, K., NIPHADKAR, P., DESHPANDE, S., BOKADE, V., Esterification of renewable levulinic acid to ethyl levulinate biodiesel catalyzed by highly active and reusable desilicated H-ZSM-5, *J. Chem. Technol. Biotechnol.*, **89**, no.10, 2014, p.1507.
4. AHMAD, E., ALAM, M.I., PANT, K. K., HAIDER, M.A., Catalytic and mechanistic insights into the production of ethyl levulinate from biorenewable feedstocks, *Green Chem.*, **18**, 2016. p. 4804.
5. KUWAHARA Y., FUJITANI T. AND YAMASHITA H., Catalytic transfer hydrogenation of biomass-derived levulinic acid and its esters to  $\gamma$ -valerolactone over  $\text{ZrO}_2$  catalyst supported on SBA-15 silica, *Catal. Today*, **237**, 2014, p.418.
6. YADAV, G. and YADAV, A., Synthesis of ethyl levulinate as fuel additives using heterogeneous solid superacidic catalysts: Efficacy and kinetic modeling, *Chem. Eng. J.*, **243**, 2014, p. 556.
7. FEYZI, M., NOROUZI, L., Preparation and kinetic study of magnetic  $\text{Ca}/\text{Fe}_3\text{O}_4@/\text{SiO}_2$  nanocatalysts for biodiesel production, *Renew Energy*, 2016, **94**, p. 580.
8. OPRESCU, E.-E., STEPAN, E., DRAGOMIR, R-E, RADU, A., ROSCA, P., Synthesis and testing of glycerol ketals as components for diesel fuel, *Fuel Process. Technol.*, **110**, 2013, p.215.
9. DOUKEH, R., TRIFOI, A., BOMBOS, M., BANU, I., PASARE, M., BOLOCAN, I., Hydrodesulfurization of Thiophene over Co, Mo and CoMo /g- $\text{Al}_2\text{O}_3$  Catalysts, *Rev. Chim.*, **69**(2), 2018, p. 396.
10. ENASCUTA, C.-E., STEPAN, E., BOLOCAN, I., BOMBOS, D., CALIN, C., OPRESCU, E.-E., LAVRIC, V., Simultaneous production of oil enriched in  $\omega$ -3 polyunsaturated fatty acids and biodiesel from fish wastes, *Waste Management*, **75**, 2018, p. 209.
11. ROPERO-VEGA, J.L., ALDANA-PÉREZA, A., GÓMEZ R., NINO-GÓMEZA, M.E., Sulfated titania [ $\text{TiO}_2/\text{SO}_4^{2-}$ ]: A very active solid acid catalyst for the esterification of free fatty acids with ethanol, *Applied Catalysis A: General*, **379**, 2010, p. 24.
12. CHEN, W.H., KO, H.H., SAKTHIVEL, A., HUANG, S.J., LIU, S.H., LO A.-Y., TSAI, T.-C., LIU, S.-B., A solid-state NMR, FT-IR and TPD study on acid properties of sulfated and metal-promoted zirconia: Influence of promoter and sulfation treatment, *Catalysis Today*, **116**, 2006, p. 115.
13. SONG, C., LAI, W. C., SCHMITZ, A. D., & REDDY, K.M., Characterization of acidic properties of microporous and mesoporous zeolite catalysts using TGA and DSC, *ACS Division of Fuel Chemistry, Preprints*, **41**, no.1, 1996, p. 72.
14. WU, T., WAN J., MA, X., Aqueous asymmetric aldol reaction catalyzed by nanomagnetic solid acid  $\text{SO}_4^{2-}/\text{Zr}(\text{OH})_4\text{-Fe}_3\text{O}_4$ , *Chinese Journal of Catalysis*, **36**, 2015, p. 429.
15. REFAAT A. A., Correlation between the chemical structure of biodiesel and its physical properties, *Int. J. Environ. Sci. Tech.*, **6**, 2009, p.680.
16. GERHARD, K., STEIDLEY, K.R., Kinematic viscosity of biodiesel fuel components and related compounds. Influence of compound structure and comparison to petrodiesel fuel components, *Fuel*, **84**, 2005, p. 1062.

Manuscript received: 3.12.2019